Temperature-corrected Performance Ratio of Grid-Connected Photovoltaic System: Tropical versus Continental Climate

Siti Nor Nadhirah Ibrahim[1], Hedzlin Zainuddin[1,2]* and Shahril Irwan Sulaiman[3]

[1]*Faculty of Applied Sciences, Universiti Teknologi MARA, 40450 Shah Alam, Selangor, Malaysia*
[2]*Faculty of Applied Sciences, SPECTRA Research Interest Group, Universiti Teknologi MARA, 40450 Shah Alam, Selangor, Malaysia*
[3]*School of Electrical Engineering, College of Engineering, Universiti Teknologi MARA, 40450 Shah Alam, Selangor, Malaysia*

ABSTRACT

Performance ratio (*PR*) is often used as a performance metric in commercial acceptance tests of an installed grid-connected photovoltaic (GCPV) system. Recently, *PR* has been claimed to significantly affect seasonal and weather variations, which would invite unnecessary risk to the commercial acceptance test. In the updated IEC 61724-1, the temperature-corrected performance ratio (*TCPR*) has been included as the performance metric to remove the seasonal and weather variations. However, not all climate regions experience these variations, which means that *TCPR* might not be necessary for certain climate regions. Due to that, this study aims to analyse the relevancy of determining *TCPR* in addition to the normal *PR* for GCPV systems for different climate regions. The analysis was conducted using PVsyst software by comparing the *PR* and *TCPR* of two similar GCPV systems: case A represents tropical climate and case B represents continental climate. The results evidently show that the *PR* and *TCPR* values are always very close for both climate regions if analysed annually. However, when analysed monthly, the normal *PR* varied significantly between 77.5% and 90.0%, indicating a 12.5% difference for continental climate, but for tropical climate, the difference is just 1.0%. Conversely, the monthly *TCPR* variation in the continental climate is insignificant, with the value ranging from 81.4% to 84.1%, indicating only a 2.7% difference. Thus, the results of this study suggest that both *PR* and *TCPR* are relevant for continental climate. However, normal *PR* alone is already sufficient for tropical climate as the performance metric.

INTRODUCTION

The solar photovoltaic (PV) energy sector has long been hailed as one of the most promising sources of electricity (Comello et al., 2018). According to the International Energy Agency (IEA), by 2027, solar PV will have exceeded coal's installed power capacity, making it the largest electricity source in the world. The cumulative solar PV capacity is forecasted to nearly triple during the forecast period, increasing by almost 1500 GW, surpassing natural gas by 2026 and coal by 2027. This achievement is due to several factors. One is utility-scale solar PV, the least expensive option for new electricity generation in most countries worldwide despite rising commodity prices. Higher retail electricity prices and growing policy support to help consumers save money on their energy bills will also spur the growth of distributed solar PV, such as rooftop solar on buildings (International Energy Agency, 2022). Solar PV industry benefits extend beyond electricity generation.

As PV capacity increases worldwide, assessing the predicted performance of solar PV systems has become significantly important to determine whether they are suitable for a particular location. Many technical and climatic factors can influence PV system performance, such as irradiation, orientation, temperature, wind speed, humidity, PV module technology, dust, and degradation. There are a few parameters used to analyse the performance of GCPV systems, which include energy production, daily yield, annual yield, seasonal yield, reference yield (Y_r), final yield (P_f), array yield (Y_A), capacity factor (CF), system efficiencies, system losses and performance ratio (Anang et al., 2021; Ibrahim et al., 2023).

Performance ratio (PR) quantifies the overall effect of losses of a GCPV system. The seven main loss factors include temperature, mismatch, soiling, ageing, shading, inverter efficiency, and cable efficiency (SEDA, 2023). Temperature is often the highest contributor to GCPV system performance loss (Dey & Subudhi, 2020; Rout & Kulkarni, 2020; Abdullah et al., 2022; Vidur & Jagwani, 2022; Ibrahim et al., 2023; Rahim et al., 2024). A study conducted by Rahim et al. (2024) in Malaysia assessed the performance of a 10 kW$_p$ GCPV system. The findings indicated that actual temperature loss could account for up to 8%, while soiling, cable, and mismatch each account for 3% losses. Mismatch accounted for an additional 2% in losses, and ageing was found to contribute the least, at 0.6%, based on simulation results. Another study was conducted in Malaysia to evaluate the performance of a 2.84 kW$_p$ GCPV system and found that the temperature loss can reach a maximum value of 14%. At the same time, 3% each of soiling and cable losses, 2% each of mismatch and inverter losses, and 0.63% of ageing and shading are assumed to be none (Ibrahim et al., 2023).

Temperature is influenced by weather and seasonal variations. Season and weather notably affect PR through ambient temperature (T_{amb}) variations, consequently influencing the PV module temperature (T_{mod}). During high T_{amb}, T_{mod} increases, causing PR to decrease and vice versa. Due to the weather and seasonal variations, PR brings forth which

locations will yield the most productive GCPV system. *PR* is often used as a benchmark value in agreement among PV system installers and owners. Unfortunately, associated with this dependence on the weather and seasons is a bias error in the metric, which introduces unnecessary risk during testing and commissioning (T&C) (Dierauf et al., 2013).

T&C is a procedure that verifies the system's safe installation and faultless operation. The acceptable *PR* is a minimum of 0.75 to pass the Reliability Run Test under T&C. The T&C procedure requires measuring GCPV system output continuously, sampled at five-minute intervals for a minimum of seven consecutive days. The data measured is defined as expected output. Historical weather data is also required to be extracted via simulation software, such as Meteonorm, Solcast and Solargis, which are defined as predicted output (MS 2692, 2020). It is fair for the PV installer and owner to specify an annualised *PR* in the contract in the T&C, giving a rough idea of how much energy the PV owner will receive for one whole year. However, the variation in season and weather of the measurement affects the annual *PR*, leading to unnecessary risk for both parties. *PR* can swing entirely over a single day. *PR* is also expected to show a significant difference based on its monthly value. For example, during summer months, *PR* is expected to be lower than in winter months due to low T_{amb} indicating underprediction, which is a risk for PV installers, while high *PR* during winter months indicates overprediction, which is a risk for PV owners (Dierauf et al., 2013).

Globally, various regions are experiencing different climates. According to Köppen-Geiger climate classification, there are five major groups of climates, including tropical (A), arid (B), temperate (C), continental (D), and polar (E), which are then divided into 30 subgroups. The first letter of the subgroups represents the type of seasonal precipitation, while the second letter represents the T_{amb} levels (Triantafyllou & Tsonis, 1994; Kottek et al., 2006; Chen & Chen, 2013; Beck et al., 2018). This study will focus on two groups, tropical and continental climates since these groups exhibit characteristics that contrast each other in terms of variations of T_{amb} throughout the year. It is important to address their climate criteria, especially T_{amb}, since this will impact the *PR* of the GCPV system installed in these climate regions. Interestingly, no subgroup of T_{amb} is defined for the tropical climate, only the precipitation, since all subgroups of tropical climate experience the minimum T_{amb} of 18°C throughout the year. The tropical climate has a small range of the monthly average of T_{amb}, which is between 25°C and 28°C (Costa et al., 2023). However, Tropical climate could notably reach an average maximum of 35°C (U.S. Department of Commerce, 2023). Conversely, the continental climate generally has an average T_{amb} of the hottest month more than 10°C and an average T_{amb} of the coldest month less than or equal to 0°C.

Previous studies have shown that seasonal and weather variations affecting *PR* can be mitigated by referencing a 25°C T_{amb} under standard test conditions (STC) (Limmanee et

al., 2016; Prakhya & Kotha, 2018; Quansah & Adaramola, 2019; Karahüseyin & Abbasoğlu, 2022; Ogliari et al., 2023; Wassie & Ahlgren, 2023). This method usually results in a higher PR because modules more frequently operate at 45°C. While it essentially solves the problem of seasonal variations, it overestimated the actual performance, thus, incapacitated PR assessment based on the effect of local climate. For that reason, correction to 25°C is not an acceptable method for removing the seasonal variability in the PR metric because it would overestimate PR.

Therefore, the National Renewable Energy Laboratory (NREL) started to highlight and introduce temperature-corrected performance ratio ($TCPR$) as a new metric to assess the performance of a GCPV system, followed by the International Electrotechnical Commission (IEC). In the updated international standard of PV monitoring, $TCPR$ was included to remove seasonal and weather variations without overestimating the actual annual PR. $TCPR$ is able to estimate the annual PR regardless of the duration of the reporting period. It is expected to discard large seasonal and weather variations by incorporating the estimated annual average module temperature (Dierauf et al., 2013; IEC 61724, 2021). Therefore, $TCPR$ is implemented by NREL and IEC61724-1:2021, introducing a power rating temperature adjustment factor ($C_{k,annual}$), which incorporates the annual average of module temperature ($T_{mod,annual-avg}$), which can be estimated by computing an irradiance-weighted average of the predicted module temperature (T_{mod}), and the value is chosen based on historical weather data for the specific site. It will reduce unnecessary risk from the effects of significantly high or significantly low T_{amb} on PR during the T&C since the $T_{mod,annual-avg}$ has been considered. It is particularly significant for climates with a wide range of annual T_{amb}, as in the continental climate. However, for the tropical climate, which experiences low annual T_{amb} variation throughout the year, the relevancy of $TCPR$ is worth questioning and further studying.

A few studies have assessed the performance of GCPV systems using $TCPR$ A study was conducted using an installed PV system in Seville, Spain. This study has applied TCPR to account for the temperature effects on two different PV module technologies, thin film and monocrystalline silicon. The application of TCPR allows for a more standardised comparison between the two technologies (Sánchez-Lanuza et al., 2024). Next, a study analysed the impact of cell temperature on the performance ratio (PR) of photovoltaic (PV) systems through experimental and numerical methods. It found that higher cell temperatures lead to decreased PR, lowering system efficiency, especially in warmer climates like the Mediterranean, where managing temperature is key to maintaining performance (De Masi et al., 2024). A study evaluated the PR and $TCPR$ of a utility-scale GCPV system under controlled spectral influences: airmass and precipitable water. The study took place in Northern Cape, South Africa, which is classified under an arid climate region. The results showed that PR is overestimated during winter and underestimated during summer. By comparing PR and

$TCPR$, $TCPR$ showed more levelized results with low monthly fluctuations for the entire year. This indicated that $TCPR$ is relevant in the arid climate region (Daniel-Durandt & Rix, 2022). Besides that, a study was conducted in Gozo, Malta, under a temperate climate region to analyse and compare 56 GCPV systems' output over one year. The systems involved ranged from residential to large-scale size. A comparison of PR and $TCPR$ showed a close value of 61% and 62%, respectively. It indicated that $TCPR$ is not relevant for performance assessment in the temperate climate region (Micallef & Staines, 2022).

Another study assessed a 3 kW$_p$ GCPV system performance located in the tropical climate region at Sakon Nakhon, Thailand. By comparing PR and $TCPR$, the results show that monthly PR has larger variations compared to $TCPR$, with standard deviations of 2.39 and 5.07, respectively. This study suggested that $TCPR$ is a relevant performance metric despite the tropical climate having low annual T_{amb} variations (Sathiracheewin et al., 2020). Conversely, research by Syahputra et al. (2018) showed that monthly PR values exhibit close variations compared to $TCPR$ with standard deviations of 5.16 and 5.17, respectively. This study suggests that $TCPR$ may not be essential for performance assessment in tropical climate regions. Additionally, a study by Gopi et al. (2021) assessed the performance of a 2 MW$_p$ GCPV system conducted in Kerala, India, which under tropical climate showed similar results of small variations to those of Syahputra et al. (2018). PR reached a maximum value of 77.56% in January and went down to 74.07% in March. At the same time, $TCPR$ varies from 77.61% to 74.88%. This result leads to the conclusion that $TCPR$ is not relevant for performance assessment in the tropical climate region. Consequently, the necessity of evaluating TCPR in continental climate regions is also called into question, given the contrasting characteristics of these two climates. It is worth highlighting that the main differences between tropical and continental climates are the fluctuations of T_{amb} and four distinct seasonal variations. The tropical climate has consistent T_{amb} throughout the year with no four distinct seasons, while the opposite is true for the continental climate. Despite comparing the value of PR and $TCPR$, this study did not quantify the deviations between these two metrics. The relevance and necessity of applying TCPR remain ambiguous and inconclusive, and a quantitative comparison of the two metrics, especially monthly, is not provided. This study seeks to address the gap in the literature by comparing the monthly and annual PR and TCPR of GCPV systems in tropical and continental regions. The analysis will be conducted using PV design and simulation software PVsyst.

METHODS

The framework of this study consists of two main parts: proving the role of $C_{k,annual}$ on the TCPR mathematical model to remove seasonal and weather variations and comparing the PR and TCPR for two case studies, as illustrated in Figure 1. The cases were the GCPV
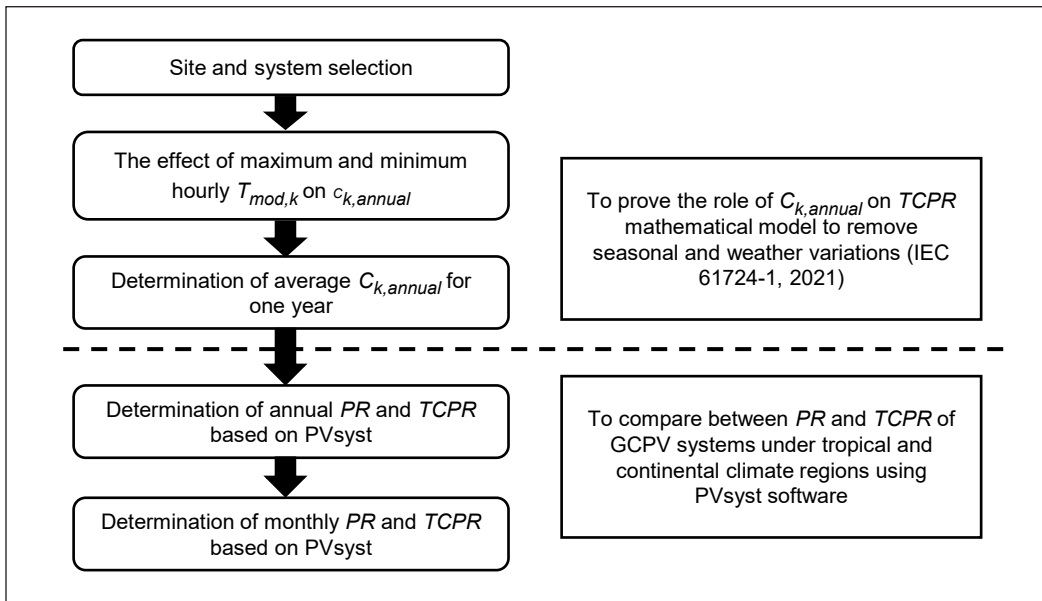
Figure 1. The study framework corresponding to the objectives

system located at Negeri Sembilan, Malaysia, under a tropical climate (referred to as Case A), and the GCPV system located at Almaty, Kazakhstan, under a continental climate (referred to as Case B).

Site and System Selection

The sites representing the two cases of tropical and continental climates were selected based on the Köppen-Geiger climate classification. Negeri Sembilan, Malaysia, has been selected to represent A_f, known as the tropical rainforest climate, while Almaty, Kazakhstan, represents D_{fa}, the hot summer continental climate with wet winters. The A_f climate is characterised by consistently high T_{amb} all year round, with the average monthly T_{amb} remaining above 18°C. There are no distinct seasonal variations, and this climate experiences substantial rainfall throughout the year without a dry season. On the other hand, the D_{fa} climate experiences a relatively hot summer, with T_{amb} frequently exceeding 30°C. Winters are cold, with T_{amb} falling below -3°C, often resulting in snowfall and frost. This climate sees more precipitation during the summer, while winters tend to be drier. Table 1 presents the selected sites with their corresponding coordinates. The two selected GCPV systems have been designed using identical technical specifications: the sizing ratio, the PV module specifications and the inverter specifications, as tabulated in Tables 2 and 3. The systems have a 10 kW_p PV array capacity and a 9 kW AC inverter. The PV modules were in 2 parallel × 20 series configurations and ground-mounted.

Table 1
Sites for different climates and their coordinates

| Case | Site | Climate | Coordinates | |
			Latitude	Longitude
A	Negeri Sembilan, Malaysia	A_f	2.7297 °N	101.9381 °E
B	Almaty, Kazakhstan	D_{fa}	43.2500 °N	76.9167 °E

Table 2
PV module specifications

Specifications	Unit	
Technology	-	Polycrystalline
Maximum power at STC	W_p	250
Open circuit voltage	V	37.47
Short circuit current	A	8.76
Maximum power voltage	V	30.34
Maximum power current	A	8.24
Temperature coefficient of voltage	$\%°C^{-1}$	-0.34
Temperature coefficient of current	$\%°C^{-1}$	0.04
Temperature coefficient of power	$\%°C^{-1}$	-0.44

Technical Performance Evaluation Based on IEC 61724-1 (2021)

There are a few parameters under technical performance evaluation based on IEC 61724-1 (2021), which include DC energy (E_A), AC energy (E_{out}), PV array energy yield (Y_A), reference yield (Y_r), final yield (Y_f), PR, and the most recent parameter, is the $TCPR$. PR can be expressed as Equation 1:

Table 3
Inverter specifications

Specifications	Unit	
Nominal power	kW	9.0
Maximum voltage	V	950
MPPT voltage	V	420..800
Maximum AC current	A	42
No. of MPPT	-	2
No. of inverter	-	1
Inverter efficiency	%	97.0

$$PR = (\frac{E_{out}}{P_0})/(\frac{H_{poa}}{G_{poa,ref}}) \qquad [1]$$

where E_{out} is the AC output energy of the PV array in the unit (kWh), P_0 is the array power rating on the DC side in the unit (kW), H_{poa} is in-plane irradiation in the unit (kWh/m^2), and $G_{poa,ref}$ is the irradiance at STC which is 1 kW/ m^2. However, PR can also be expressed as Equation 4 by expanding E_{out} as Equation 2 and H_{poa} as Equation 3 and moving P_0 to the denominator:

$$E_{out} = \sum_k P_{out,k} \times \tau_k \qquad [2]$$

$$H_{poa} = \sum_k G_{poa,k} \times \tau_k \qquad [3]$$

$$PR = (\sum_k P_{out,k} \times \tau_k)/(\sum_k (\frac{P_0 \times G_{poa,k} \times \tau_k}{G_{poa,ref}})) \qquad [4]$$

where P_{out} is the power output at the AC side, G_{poa} is in-plane irradiance in unit (kW/ m²), and τ is the time interval at the kth recording interval within a reporting period in unit (h). On the other hand, $TCPR$ can be expressed as Equation 5:

$$TCPR = (\sum_k P_{out,k} \times \tau_k)/(\sum_k (\frac{(C_{k,annual} \times P_0) \times G_{poa,k} \times \tau_k}{G_{poa,ref}})) \qquad [5]$$

where $C_{k,annual}$ is the power rating temperature adjustment factor. It is the unique and distinctive parameter added to the previous PR equation and becomes the TCPR parameter. This parameter serves to account for monthly temperature variations in a GCPV system by normalising or evening out the monthly PR throughout the year. It achieves this by compensating for the impact of temperature changes across different seasons and weather conditions using the annual average module temperature $T_{mod,annual-avg}$. Since TCPR is designed to estimate the annual PR regardless of the reporting period's length, all $T_{mod,k}$ values in the TCPR calculations are balanced or neutralised by the $T_{mod,annual-avg}$, ensuring consistency in each interval calculation. The side-by-side comparison between PR and TCPR is tabulated in Table 4.

Table 4
Comparison between PR and TCPR mathematical model

PR	TCPR
$PR = \frac{(\sum_k P_{out,k} \times \tau_k)}{P_0} / \frac{\sum_k G_{poa,k} \times \tau_k}{G_{poa,ref}}$	$TCPR = \frac{(\sum_k P_{out,k} \times \tau_k)}{P_0} / \frac{\sum_k (C_{k,annual} \times G_{poa,k}) \times \tau_k}{G_{poa,ref}})$
	$C_k = 1 + \gamma \times (T_{mod,k} - T_{mod,annual-avg})$
	$T_{mod,annual-avg} = \sum (G_{poa,k} \times T_{mod,k})/\sum (G_{poa,k})$

$C_{k,annual}$ Determination

$C_{k,annual}$ is expected to play a role in removing seasonal and weather variations since it is the power rating temperature adjustment factor. To ensure the $TCPR$ concept is applied correctly, the value of the annual $TCPR$ should be close to the value of the annual PR. Despite the fact that $TCPR$ is expected to correct the monthly PR seasonal and weather variations, $TCPR$ will not overestimate or underestimate the annual PR. Since $C_{k,annual}$ is the only parameter distinguishing between $TCPR$ and PR, mathematically $C_{k,annual}$ should

be approximately one. $C_{k,annual}$ can be expressed as Equation 6:

$$C_{k,annual} = 1 + \gamma \times (T_{mod,k} - T_{mod,annual-avg})$$ [6]

where γ is the relative maximum-power temperature coefficient in unit °C⁻¹, $T_{mod,annual-avg}$ is the annual average PV module temperature in unit °C chosen based on historical weather data for the site. It should be calculated by computing an irradiance-weighted average of the predicted module temperature (T_{mod}) in unit °C which can be expressed as Equation 7:

$$T_{mod,annual-avg} = \sum (G_{poa,k} \times T_{mod,k}) / \sum (G_{poa,k})$$ [7]

$T_{mod,annual-avg}$ is kept constant throughout the monthly calculation of $TCPR$.

In the interest of proving the $TCPR$ concept, the effect of maximum and minimum hourly $T_{mod,k}$ on $C_{k,annual}$ is calculated. Firstly, the hourly raw data was obtained from Solcast for one year (https://toolkit.solcast.com.au/). Table 5 presents the sample of raw data obtained from Solcast between 8 a.m. and 7 p.m. for every hour on the 5th of February 2023 for Case A. Next, the raw data took into account daytime data based on the filtration of $G_{poa} \geq 40$ W/m² due to T_{amb} and T_{mod} reaching an equilibrium state when the G_{poa} reached 40 W/m² (Zainuddin, 2014). Then, the T_{mod} was calculated for every hour for one year. For Case A, this study has applied Zainuddin's (2014) mathematical model, which can be expressed as Equation 8, to calculate T_{mod}, while for Case B, the Tamizhmani et al. (2003) mathematical model was applied, which can be expressed as Equation 9.

$$T_{mod} = -8.58 + 0.02\,G_{poa} + 1.53\,T_{amb} - 0.58\,WS - 0.05\,RH$$ [8]

Table 5
Environment data sample extracted from Solcast

Date	Period	Time	T_{amb} (°C)	G_{poa} (W/m²)	RH (%)	WS (ms⁻¹)
5/2/2023	60min	8:00:00 AM	25	47	95.6	1.8
5/2/2023	60min	9:00:00 AM	26	237	89.9	1.8
5/2/2023	60min	10:00:00 AM	29	460	79.1	1.6
5/2/2023	60min	11:00:00 AM	31	658	70.9	1.8
5/2/2023	60min	12:00:00 PM	32	805	66	1.9
5/2/2023	60min	1:00:00 PM	33	876	61.4	1.8
5/2/2023	60min	2:00:00 PM	34	883	58.5	1.8
5/2/2023	60min	3:00:00 PM	33	647	62.3	1.8
5/2/2023	60min	4:00:00 PM	32	533	66.1	1.7
5/2/2023	60min	5:00:00 PM	32	198	66.2	1.3
5/2/2023	60min	6:00:00 PM	30	101	71.9	1.2
5/2/2023	60min	7:00:00 PM	28	44	80.7	1.2

$$T_{mod} \; = \; 4.3 + 0.028\,G_{poa} + 0.943\,T_{amb} - 1.528\,WS \qquad [9]$$

WS is the wind speed in the unit (ms^{-1}), and RH is the relative humidity in the unit (%). Afterwards, $T_{mod,annual-avg}$ can be calculated using Equation 7. Lastly, $C_{k,annual}$ was calculated for every hour for one year using Equation 6. The maximum and minimum hourly $T_{mod,k}$, with the respective $C_{k,annual}$, were identified from the one-year data.

Next, the average $C_{k,annual}$ for one year was determined using the same hourly $C_{k,annual}$ data obtained from Solcast. However, instead of assessing the extreme value of $T_{mod,k}$, the yearly average $C_{k,annual}$ has been calculated by averaging the hourly $C_{k,annual}$ for one year. It is to observe the result of $C_{k,annual}$ on a yearly basis.

Comparison Between *PR* and *TCPR* Using PVsyst Simulation

The comparison between *PR* and *TCPR* using PVsyst software involved GCPV systems simulation for cases of tropical and continental climates. The comparison was divided into two main sections: the determination on an annual basis and the determination on every month. The PVsyst simulation has been done by incorporating the mentioned sites and systems selection. The simulation design parameters were kept constant except for meteorological data selection that will represent each climate respectively. PVsyst offers a few meteorological databases, including Meteonorm 8.1, NASA-SSE, PVGIS TMY, NREL, Solcast TMY and SolarAnywhere. Users are allowed to upload their raw data if it matches the PVsyst format. This study selected Meteonorm 8.1 due to its accuracy in in-plane solar irradiation (H_{poa}) data compared to others (Rahim et al., 2024). PVsyst is able to simulate technical, economic, and environmental performance. However, this study is limited to the boundary of technical performance only. Running PVsyst simulation requires the user to incorporate various losses that are expected to affect the GCPV system. These losses were also determined carefully and kept constant for both climates to ensure a fair comparison. Table 6 presents the losses applied in the PVsyst simulation (PVsyst SA, 2024).

The PV array orientations have been selected thoughtfully for both sites since this is a fixed tilt system to avoid losses and ensure a fair comparison between the two climate regions. The tilt angle of a PV array is one of the crucial aspects of harvesting maximum irradiance (Tahsin, 2021). The tilt angle of the PV array was determined by following the rule of thumb, which is based on the latitude of the sites selected (Chen et al., 2018; Chinchilla et al., 2021). For case A, supposedly, the tilt angle is 3°. However, for sites with a latitude of less than 10°, the optimal tilt angle would be 10° to allow rain to naturally wash the PV modules (Jacobson & Jadhav, 2018). For case B, supposedly, the tilt angle is 43°; even so, considering this study used PVsyst as a simulation tool to assess the performance of the GCPV system, the loss with respect to the optimum features in PVsyst

was considered. Therefore, the tilt angle was adjusted to reach 0% loss. Hence, the tilt angle is 40°. The azimuth angle simply depends on which hemisphere the sites are located in: southern hemisphere: 0° facing north and northern hemisphere: 0° facing south. Table 7 summarises the tilt angle and azimuth angle for both cases.

Table 6
GCPV system losses in PVsyst

No.	Losses	Values	Description/Assumption
1	Field thermal loss factor	29.0 W/m²K	PVsyst default value (Assuming that the PV array mounting is open rack)
2	Ohmic loss	1.5%	PVsyst default value
3	Module quality	-0.5%	PVsyst default value
4	Light-induced degradation	2.0%	PVsyst default value
5	Module mismatch loss	2.0%	PVsyst default value
6	Strings voltage mismatch	0.15%	PVsyst default value
7	Yearly soiling loss factor	3.0%	PVsyst default value
8	Incidence angle modifier	1.8%	Based on the PV module datasheet
9	Ageing	0%	The system is new (assuming for new installation)
10	Shading loss	0%	Assuming the system is free from shading.

Table 7
GCPV system orientation

Case	Sites	Climate	Tilt angle	Azimuth angle
A	Negeri Sembilan, Malaysia	A_f	10°	0° facing south
B	Almaty, Kazakhstan	D_{fa}	40°	0° facing south

RESULTS AND DISCUSSION

The results are divided into two parts to satisfy the research objectives. The first objective is to prove the role of $C_{k,annual}$ in the *TCPR* mathematical model to remove seasonal and weather variations (IEC 61724-1, 2021). The second objective is to compare the *PR* and *TCPR* of GCPV systems under tropical and continental climate regions using PVsyst software.

The Effect of Maximum and Minimum Hourly T_{mod} on $C_{k,annual}$

$C_{k,annual}$ was calculated by incorporating the maximum and minimum hourly $T_{mod,k}$ into the calculation. The effect of extreme hourly PV module temperatures was analysed to prove the *TCPR* concept of removing seasonal and weather variations. Based on the *PR* and *TCPR* equations, the difference is just adding the $C_{k,annual}$ parameter into the normal *PR* equation and is later addressed as *TCPR* (Dierauf et al., 2013; IEC 61724, 2021). This

means $C_{k,annual}$'s value should be approximately one ($C_{k,annual} \approx 1$), so *PR* and *TCPR* are close. $C_{k,annual}$ has been calculated to verify that the *TCPR* concept was applied correctly using raw data extracted from Solcast for tropical and continental climate regions. Table 8 presents the environmental data pertaining to the highest and the lowest T_{mod} of the year based on average hourly data with $C_{k,annual}$ for Case A, while Table 9 for Case B.

Table 8
Extreme T_{mod} (°C) and the $C_{k,annual}$ for Case A

Date	Time	T_{amb} (°C)	G_{poa} (W/m²)	$T_{mod,k}$ (°C)	$T_{mod,annual-avg}$ (°C)	$C_{k,annual}$
2023-05-02	2:00:00 PM	34	883	57.13	43.50	0.94
2023-02-06	9:00:00 AM	23	53	21.64		1.10

Table 9
Extreme T_{mod} (°C) and the $C_{k,annual}$ for Case B

Date	Time	T_{amb} (°C)	G_{poa} (W/m²)	$T_{mod,k}$ (°C)	$T_{mod,annual-avg}$ (°C)	$C_{k,annual}$
2023-07-26	1:00:00 PM	31	972	57.08	31.92	0.89
2023-01-13	8:00:00 AM	-25	42	-21.31		1.23

For Case A, the highest T_{mod} was 57.13°C, resulting in $C_{k,annual}$ being 0.94, while the lowest T_{mod} was 21.64°C, resulting in $C_{k,annual}$ being 1.10. On the other hand, for Case B, the highest T_{mod} was 57.08°C, resulting in $C_{k,annual}$ being 0.89, while the lowest T_{mod} was -21.31°C, resulting in $C_{k,annual}$ being 1.23. When T_{mod} is more than $T_{mod,annual-avg}$, $C_{k,annual}$ will be less than 1 and vice versa. During cases where $C_{k,annual}$ is equal to one, there is no temperature adjustment or removal of seasonal variations on *PR*. These results portray the role or contribution of $C_{k,annual}$ in the *TCPR* equation mathematically to remove seasonal and weather variation encountered previously in normal *PR*. Thus, *TCPR* is anticipated to treat seasonal and temperature variations monthly and yearly.

Determination of Average $C_{k,annual}$ for One Year

The average $C_{k,annual}$ for one year has been calculated and presented in Table 10. Compared to extreme T_{mod}, on a yearly basis, both cases show that $C_{k,annual}$ is closer to one. During extreme T_{mod}, the power rating has been adjusted to compensate for the differences between the maximum or minimum T_{mod} and the $T_{mod,annual-avg}$. For the annual average, there is no adjustment since there is no difference between the T_{mod} (yearly) and $T_{mod,annual-avg}$. This means that while $C_{k,annual}$ reduces seasonal and weather variations on monthly *TCPR*, it does not affect yearly. Thus, the *TCPR* concept of removing seasonal and weather variations without overestimating the annual *PR* has been done in accordance with IEC 61724-1 (2021).

Table 10
Yearly average $C_{k,annual}$

Case	Site	Climate	$T_{mod,annual-avg}$ (°C)	$C_{k,annual}$
A	Negeri Sembilan, Malaysia	A_f	43.50	**1.02**
B	Almaty, Kazakhstan	D_{fa}	31.92	**1.03**

Determination of Annual *PR* and *TCPR* Based on PVsyst

Next, the annual *PR* and *TCPR* were extracted from PVsyst, and the mean bias error (MBE) for both parameters was calculated. PVsyst calculates *PR* and *TCPR* based on IEC 61724-1 (2021), as stated in the PVsyst help content. Figure 2 illustrates the graph of *PR* and *TCPR* against climate with their MBE to compare annual *PR* and annual *TCPR* for tropical and continental climate regions.

The values of the annual *PR* and annual *TCPR* are close to each other for both climates. The positive MBE indicates *TCPR* is higher than *PR*, while the negative MBE is vice versa. This indicates that the *TCPR* concept of removing seasonal and weather variations without overestimating the actual *PR* is proven.
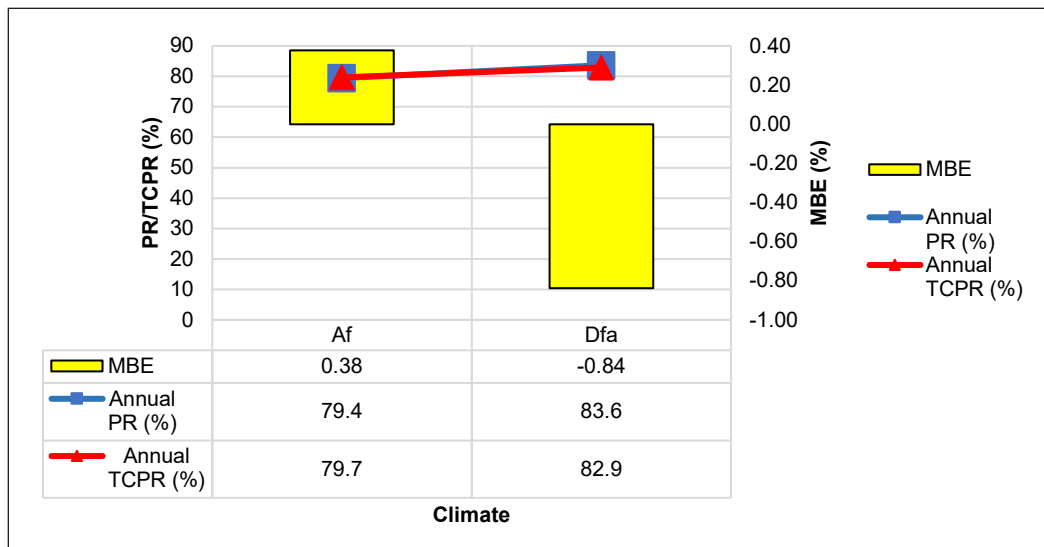

	Af	Dfa
MBE	0.38	-0.84
Annual PR (%)	79.4	83.6
Annual TCPR (%)	79.7	82.9

Figure 2. Annual comparison between *PR* and *TCPR* for Case A and Case B

Determination of Monthly *PR* and *TCPR* Based on PVsyst

Analysis of monthly *PR* and monthly *TCPR* extracted from PVsyst has been conducted to observe the effect of seasonal and weather variations on *PR*, focusing especially on monthly T_{amb}. Table 11 tabulates the monthly data for Case A, including the H_{poa}, T_{amb}, E_{out}, *PR* and *TCPR*, while Figure 3 illustrates the result in a graph.

Table 11
Monthly data for Case A

| Month	H_{poa} (kWh/m²)	T_{amb} (°C)	E_{out} (kWh)	PR (%)	TCPR (%)
Jan	159.7	27.03	1272	79.7	80
Feb	164.3	27.67	1305	79.4	80.4
Mar	170.2	27.99	1348	79.2	80.1
Apr	158.8	27.68	1257	79.1	79.8
May	146.9	28.41	1159	78.9	79.3
Jun	125.1	27.92	993	79.4	79
Jul	133.5	27.91	1059	79.4	79.1
Aug	141.4	27.78	1125	79.5	79.5
Sep	141.3	27.2	1121	79.4	79.5
Oct	147.8	27.58	1175	79.5	79.8
Nov	136.9	26.68	1093	79.8	79.9
Dec	137.5	26.99	1094	79.6	79.8
Year	1763.4	27.57	14001	79.4	79.7
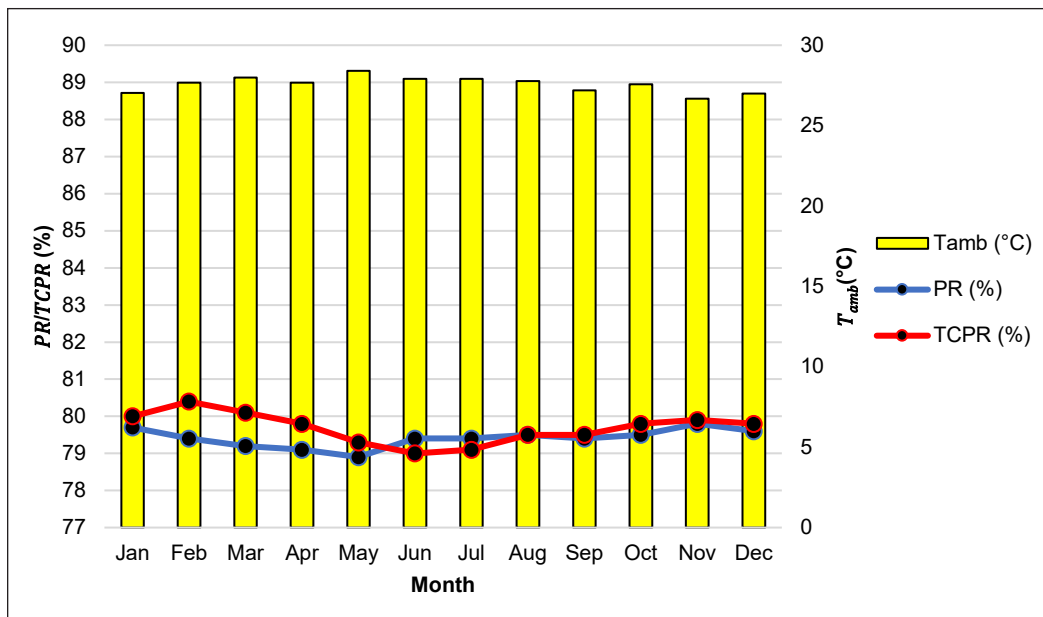
Figure 3. Monthly comparison of *PR* and *TCPR* for Case A

Based on Figure 3, the *TCPR* line trend is in good agreement with the *PR* line throughout the year, with minor deviations. The minimum *PR* recorded was in May, with 78.9% during the highest T_{amb} of 28.41°C. The corresponding *TCPR* was 79.3%. *TCPR* has adjusted the seasonal and weather variations by increasing the value; thus, the value is levelized with other months. The maximum *PR* recorded was in August, with 79.8% during

the lowest T_{amb} of 26.68°C. *TCPR* has adjusted for the seasonal and weather variations by decreasing the value; thus, the value is levelized with other months. However, the difference between *PR* and *TCPR* is found to be insignificant. This indicates that *TCPR* is not relevant in tropical climate regions.

On the other hand, Table 12 presents the monthly data for Case B, including the H_{poa}, T_{amb}, E_{out}, *PR* and *TCPR*, while Figure 4 illustrates the results in a graph.

Table 12
Monthly data for Case B

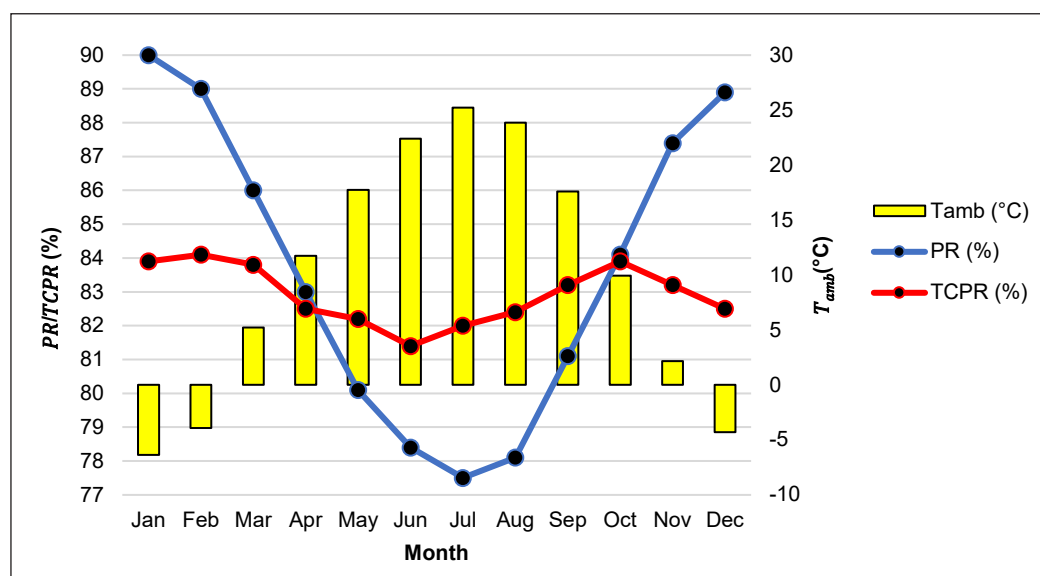| Month	H_{poa} (kWh/m²)	T_{amb} (°C)	E_{out} (kWh)	*PR* (%)	TCPR (%)
Jan	91.3	-6.36	822	90	83.9
Feb	108.7	-3.92	968	89	84.1
Mar	146.2	5.23	1258	86	83.8
Apr	141.6	11.73	1176	83	82.5
May	172.6	17.74	1383	80.1	82.2
Jun	161.4	22.4	1265	78.4	81.4
Jul	180.7	25.21	1401	77.5	82
Aug	176.8	23.85	1381	78.1	82.4
Sep	163.3	17.58	1325	81.1	83.2
Oct	132.1	9.94	1111	84.1	83.9
Nov	81.7	2.16	714	87.4	83.2
Dec	64.7	-4.3	575	88.9	82.5
Year	1621.1	10.11	13379	83.6	82.9

Figure 4. Monthly comparison of *PR* and *TCPR* for Case B

Based on Figure 4, the *PR* line is interestingly curved like a U-shape, indicating that the monthly values are in a larger range throughout the year. There is a distinct difference between maximum and minimum monthly values. Inversely, the *TCPR* line is more balanced, indicating a small difference between maximum and minimum monthly values. Thus, *TCPR* is levelized for every month. The minimum *PR* recorded was in July, with 77.5% during the highest T_{amb} of 25.21°C. The corresponding *TCPR* was 82%. *TCPR* has adjusted the seasonal and weather variations by increasing the value by 4.5%; thus, the value level is revised with other months. The maximum *PR* recorded was in August, at 90.0%, during the lowest T_{amb} at -6.36°C. The corresponding *TCPR* was 83.9%. *TCPR* has adjusted the seasonal and weather variations by decreasing the value by 6.1%; thus, the value levelized with other months. It is apparent that the difference between *PR* and *TCPR* is significant. It is worth highlighting that *TCPR* is relevant in the continental climate region.

The minimum *PR* (PR_{min}), maximum *PR* (PR_{max}), minimum *TCPR* ($TCPR_{min}$), and maximum *TCPR* ($TCPR_{max}$) are summarised in Table 13 for both cases. The PR_{diff} and $TCPR_{diff}$ were also calculated by subtracting the maximum and minimum of the respective parameters. The purpose of obtaining the PR_{diff} and $TCPR_{diff}$ was to observe the range or variations of the monthly values, which was highly expected due to season or weather. Large PR_{diff} or $TCPR_{diff}$ indicates large variations and the other way around for small values. PR_{diff} and $TCPR_{diff}$ should be compared to see the effectiveness of applying *TCPR*.

For Case A, the range of monthly *PR* is between 78.9% and 79.8%, indicating a 1% PR_{diff}. The range of monthly *TCPR* is between 79.0% and 80.4%, indicating a 1.3% $TCPR_{diff}$. Since the difference between PR_{diff} and $TCPR_{diff}$ is small, there is minimal risk of seasonal and weather variations. Thus, this case study has highlighted that *PR* assessment is sufficient without the *TCPR* assessment for the tropical climate region.

For Case B, the range of monthly *PR* is between 77.5% and 90.0%, indicating a 12.5% PR_{diff}. The range of monthly *TCPR* is between 81.4% and 84.1%, indicating a 2.7% $TCPR_{diff}$. Since PR_{diff} is large, seasonal and weather variations are significantly risky. The range of $TCPR_{diff}$ significantly reduced compared to PR_{diff}. Thus, this case study has proven that the implementation of *TCPR*, as recommended by IEC 61724-1 (2021), is relevant for the continental climate region due to the wide range of annual T_{amb}.

Table 13

Analysis of monthly PR and TCPR

Case	PR_{min} (%)	PR_{max} (%)	PR_{diff} (%)	$TCPR_{min}$ (%)	$TCPR_{max}$ (%)	$TCPR_{diff}$ (%)	$TCPR_{diff} - PR_{diff}$ (%)
A	78.9	79.9	1	79	80.4	1.3	-0.3
B	77.5	90	12.5	81.4	84.1	2.7	9.8

CONCLUSION

$C_{k,annual}$ is determined by incorporating $T_{mod,annual-avg}$, which is actually the irradiance-weighted PV module temperature. For the tropical climate, the hourly highest and lowest T_{mod} analysis resulted in $C_{k,annual}$ of 0.94 and 1.10, respectively. On the other hand, for the continental climate, the analysis of hourly highest and lowest T_{mod} resulted in $C_{k,annual}$ of 0.89 and 1.23, respectively. These results indicate that $C_{k,annual}$ varies significantly with hourly extreme T_{mod}. However, when analysed annually, the $C_{k,annual}$ for both climates are 1.02 and 1.03. It has been proven that $C_{k,annual}$ role in removing seasonal and weather variations in the $TCPR$ mathematical model is successful for both climates.

The annual PR and $TCPR$ have no notable difference for tropical and continental climates. Nevertheless, the monthly PRs have shown obvious variations ranging from 77.5% to 90% for the continental climate. However, when $TCPR$ is applied, the variation is in the range of 81.4% to 84.1%, which is considered small. It is due to the $C_{k,annual}$ role in removing seasonal and weather variations in the $TCPR$ mathematical model. For tropical climate, it is interesting to highlight that the monthly PRs have no obvious variations ranging from 78.9% to 79.8%. The same results appear for monthly TCPR, which ranges from 79% to 80.4%. Thus, the results of this study acknowledge that both PR and $TCPR$ are relevant for the continental climate. However, normal PR alone is already sufficient for tropical climate as the performance metric.

ACKNOWLEDGEMENT

REFERENCES

Abdullah, A. Z., Amlus, M. H., Azizan, N., Sali, I. M., & Rahim, M. H. (2022). Performance analysis of different type PV module for 3kW residential roof top PV system using PVSyst simulation tool. *Journal of Physics: Conference Series*, *2312*(1), Article 012042. https://doi.org/10.1088/1742-6596/2312/1/012042

Anang, N., Azman, S. N. A. S. N., Muda, W. M. W., Dagang, A. N., & Daud, M. Z. (2021). Performance analysis of a grid-connected rooftop solar PV system in Kuala Terengganu, Malaysia. *Energy and Buildings*, *248*, Article 111182. https://doi.org/10.1016/j.enbuild.2021.111182

Beck, H. E., Zimmermann, N. E., McVicar, T. R., Vergopolan, N., Berg, A., & Wood, E. F. (2018). Present and future köppen-geiger climate classification maps at 1-km resolution. *Scientific Data, 5*(1), 1-12. https://doi.org/10.1038/sdata.2018.214

Chen, D., & Chen, H. W. (2013). Using the Köppen classification to quantify climate variation and change: An example for 1901-2010. *Environmental Development*, *6*(1), 69–79. https://doi.org/10.1016/j.envdev.2013.03.007

Chen, X. M., Li, Y., Zhao, Z. G., Ma, T., & Wang, R. Z. (2018). General method to obtain recommended tilt and azimuth angles for photovoltaic systems worldwide. *Solar Energy*, *172*, 46–57. https://doi.org/10.1016/j.solener.2018.06.045

Chinchilla, M., Santos-Martín, D., Carpintero-Rentería, M., & Lemon, S. (2021). Worldwide annual optimum tilt angle model for solar collectors and photovoltaic systems in the absence of site meteorological data. *Applied Energy, 281*, Article 116056. https://doi.org/10.1016/j.apenergy.2020.116056

Comello, S., Reichelstein, S., & Sahoo, A. (2018). The road ahead for solar PV power. In *Renewable and Sustainable Energy Reviews* (Vol. 92, pp. 744–756). Elsevier Ltd. https://doi.org/10.1016/j.rser.2018.04.098

Costa, H., Sprout, E., Teng, S., McDaniel, M., Hunt, J., Boudrea, D., Ramroop, T., Rutledge, K., & Hall, H. (2023). Tropics. In J. Evers, K. West, & Emdash Editing (Eds.), *National Geographic*. National Geographic Society.

Daniel-Durandt, F., & Rix, A. (2022). Spectral influences on performance: A South African PV plant after 4 years of operation. In *2022 International Conference on Electrical, Computer, Communications and Mechatronics Engineering (ICECCME)* (pp. 1-6). IEEE Publishing. https://doi.org/10.1109/ICECCME55909.2022.9988688

De Masi, R. F., Gigante, A., Ruggiero, S., & Vanoli, G. P. (2024). Experimental and numerical approach for the evaluation of PV-system performance on energy and environmental behavior of nearly zero energy buildings: Case study in Mediterranean climate. *Renewable Energy*, *227*, Article 120609. https://doi.org/10.1016/j.renene.2024.120609

Dey, D., & Subudhi, B. (2020). Design, simulation and economic evaluation of 90 kW grid connected Photovoltaic system. *Energy Reports*, *6*, 1778–1787. https://doi.org/10.1016/j.egyr.2020.04.027

Dierauf, T., Growitz, A., Kurtz, S., Becerra, J. L., Fichtner, C., Riley, E., & Hansen, C. (2013). *Weather-Corrected Performance Ratio*. U.S. Department of Energy. http://www.osti.gov/bridge

Gopi, A., Sudhakar, K., Keng, N. W., & Krishnan, A. R. (2021). Comparison of normal and weather corrected performance ratio of photovoltaic solar plants in hot and cold climates. *Energy for Sustainable Development*, *65*, 53–62. https://doi.org/10.1016/j.esd.2021.09.005

Ibrahim, S. N. N., Zainuddin, H., Rahim, Y. I. A. A., Mansor, N. A., Muhammad, N., & Khir, F. L. M. (2023). Simulation and prediction of residential grid-connected photovoltaic system performance. *International Journal of Power Electronics and Drive Systems*, *14*(1), 506-515. https://doi.org/10.11591/ijpeds.v14.i1.pp506-515

IEC 61724. (2021). *International Standard*. International Electrotechnical Commission. www.iec.ch

International Energy Agency. (2022). *Renewables 2022 Analysis and Forecast to 2027*. International Energy Agency. www.iea.org

Jacobson, M. Z., & Jadhav, V. (2018). World estimates of PV optimal tilt angles and ratios of sunlight incident upon tilted and tracked PV panels relative to horizontal panels. *Solar Energy*, *169*, 55–66. https://doi.org/10.1016/j.solener.2018.04.030

Karahüseyin, T., & Abbasoğlu, S. (2022). Performance loss rates of a 1 MWp PV plant with various tilt angle, orientation and installed environment in the capital of Cyprus. *Sustainability*, *14*(15), Article 9084. https://doi.org/10.3390/su14159084

Kottek, M., Grieser, J., Beck, C., Rudolf, B., & Rubel, F. (2006). World map of the Köppen-Geiger climate classification updated. *Meteorologische Zeitschrift*, *15*(3), 259–263. https://doi.org/10.1127/0941-2948/2006/0130

Limmanee, A., Udomdachanut, N., Songtrai, S., Kaewniyompanit, S., Sato, Y., Nakaishi, M., Kittisontirak, S., Sriprapha, K., & Sakamoto, Y. (2016). Field performance and degradation rates of different types of photovoltaic modules: A case study in Thailand. *Renewable Energy*, *89*, 12–17. https://doi.org/10.1016/j.renene.2015.11.088

Micallef, A., & Staines, C. S. (2022). Generation performance analysis for installed photovoltaic systems on the Maltese Islands. In *2022 Workshop on Blockchain for Renewables Integration (BLORIN)* (pp. 74-79). IEEE Publishing. https://doi.org/10.1109/BLORIN54731.2022.10028183

MS 2692. (2020). *Testing and Commissioning of Grid-Connected Photovoltaic System*. Department of Standards Malaysia. http://www.jsm.gov.my

Ogliari, E., Dolara, A., Mazzeo, D., Manzolini, G., & Leva, S. (2023). Bifacial and monofacial PV systems performance assessment based on IEC 61724-1 standard. *IEEE Journal of Photovoltaics*, *13*(5), 756–763. https://doi.org/10.1109/JPHOTOV.2023.3295869

Prakhya, R. K., & Kotha, S. R. (2018). Temperature effect on the performance metrics of gridtied SPV plant. *International Journal of Engineering Research and Technology, 11*(6), 909-923. http://www.irphouse.com

PVsyst SA. (2024). *PVsyst 7.4 - Photovoltaic System Study*. PVsyst SA. https://www.pvsyst.com/help/index.html?contents_table.htm

Quansah, D. A., & Adaramola, M. S. (2019). Assessment of early degradation and performance loss in five co-located solar photovoltaic module technologies installed in Ghana using performance ratio time-series regression. *Renewable Energy*, *131*, 900–910. https://doi.org/10.1016/j.renene.2018.07.117

Rahim, Y. I. A. A., Zainuddin, H., Setiawan, E. A., Madsuha, A. F., Hussin, M. Z., Sulaiman, S. I., & Ibrahim, S. N. N. (2024). Performance of grid-connected photovoltaic systems in Northern and Southern Hemispheres under equatorial climate. *International Journal of Power Electronics and Drive Systems*, *15*(2), 858–873. https://doi.org/10.11591/ijpeds.v15.i2.pp858-873

Rout, K. C., & Kulkarni, P. S. (2020). Design and performance evaluation of proposed 2 kW solar PV rooftop on grid system in Odisha using PVsyst. In *2020 IEEE International Students' Conference on Electrical, Electronics and Computer Science (SCEECS)* (pp. 1-6). IEEE Publishing. https://doi.org/10.1109/SCEECS48394.2020.124

Sánchez-Lanuza, M. B., Lillo-Bravo, I., Moreno-Tejera, S., Rodríguez, J. S., & Delgado-Sanchez, J. M. (2024). Experimental CIGS technology performance under low concentration photovoltaic conditions. *Journal of Cleaner Production, 446*, Article 141384. https://doi.org/10.1016/j.jclepro.2024.141384

Sathiracheewin, S., Sripadungtham, P., & Kamuang, S. (2020). Performance analysis of grid-connected PV Rooftop, at Sakon Nakhon Province, Thailand. *Advances in Science, Technology and Engineering Systems*, *5*(4), 816–823. https://doi.org/10.25046/AJ050496

SEDA. (2023). *Design and Sizing of Grid-connected Photovoltaic Power System* (3rd ed.). SEDA Malaysia. www.seda.gov.my

Syahputra, E., Fajarin, R. A., & Setiawan, E. A. (2018). Characteristic analysis of photovoltaic on-grid system in tropical region for weather-corrected performance ratio calculation method implementation. In *E3S Web of Conferences* (Vol. 67, p. 01025). EDP Sciences. https://doi.org/10.1051/e3sconf/20186701025

Tahsin, A. (2021). *Tilt angle optimization of photovoltaic modules considering the effect of dust.* [Master dissertation]. Bangladesh University of Engineering and Technology, Bangladesh. http://lib.buet.ac.bd:8080/xmlui/bitstream/handle/123456789/6062/Full%20Thesis.pdf?sequence=1&isAllowed=y

Tamizhmani, G., Ji, L., Tang, Y., Petacci, L., & Osterwald, C. (2003). Photovoltaic module thermal/wind performance: Long-term monitoring and model development for energy rating. In *NCPV and Solar Program Review Meeting Proceedings* (No. NREL/CP-520-35645). National Renewable Energy Laboratory.

Triantafyllou, G. N., & Tsonis, A. A. (1994). Assessing the ability of the Koppen system to delineate the general world pattern of climates. *Geophysical Research Letters*, *21*(25), 2809–2812.

U.S. Department of Commerce. (2023). *Tropical Weather Systems*. National Oceanic and Atmospheric Administration. https://www.noaa.gov/jetstream/tropical

Vidur, P. R., & Jagwani, S. (2022). Design and simulation of a Rooftop solar PV system Using PV syst software. In *2022 4th International Conference on Smart Systems and Inventive Technology (ICSSIT)* (pp. 724-728). IEEE Publishing. https://doi.org/10.1109/icssit53264.2022.9716348

Wassie, Y. T., & Ahlgren, E. O. (2023). Performance and reliability analysis of an off-grid PV mini-grid system in rural tropical Africa: A case study in southern Ethiopia. *Development Engineering*, *8*, Article 100106. https://doi.org/10.1016/j.deveng.2022.100106

Zainuddin, H. (2014). *Module Temperature Modelling for Free-Standing Photovoltaic System in Equatorial Climate.* [Doctoral dissertation]. Universiti Teknologi MARA, Malaysia. https://ir.uitm.edu.my/id/eprint/16413/